Acetylation of a Heterocyclic Enaminonitrile: Unambiguous Structural Assignment using NMR Methods

Colin P. Dell, Trevor J. Howe and Will G. Prowse*

Lilly Research Centre Limited, Eli Lilly and Company, Windlesham, Surrey, GU20 6PH, UK.

Received September 1, 1993

Using a combination of nmr techniques, the structure of the acetylation product of methyl 3-[2-amino-3-cyano-9-methoxy-4*H*-5,6-dihydronaphtho[1,2-*b*]pyran-4-yl] benzoate **2b** has been shown to be the *N*-acetyl derivative **5a**, rather than the rearranged 2-acetoxydihydropyridine **6a**.

J. Heterocyclic Chem., **31**, 749 (1994).

The addition of active methylene compounds to enones can yield a variety of interesting cyclic products, for example pyrans [1], dihydropyridones [2], pyridines [1,3], arenes [4], cycloalkanes [4], depending on the reaction conditions employed and on the nature of the active methylene component. One of our current interests lies in a class of compounds, the 2-amino-4-aryl-4*H*-5,6-dihydronaphtho[1,2-*b*]pyran-3-carbonitriles **2** prepared in just such a manner (Scheme 1) following the pioneering work of Otto [1].

1a $R^1=R^2=H$

1b $R^1=OMe$, $R^2=CO_2Me$

2a $R^1=R^2=H$

2b $R^1=OMe$, $R^2=CO_2Me$

SCHEME 1

Of some interest in the publications of Otto's group were the observations that under appropriate conditions this same mixture of malononitrile and Michael acceptor could yield alkoxypyridines **3** (Scheme 2). Indeed, a mechanism was proposed [1] in which the pyran **2a** was believed to be a precursor to the pyridine **3**, this conversion occurring through Dimroth rearrangement and subsequent disproportionation. Some evidence for this route was presented as treatment of the pyran **2a** with alkoxide apparently produced the product **3**.

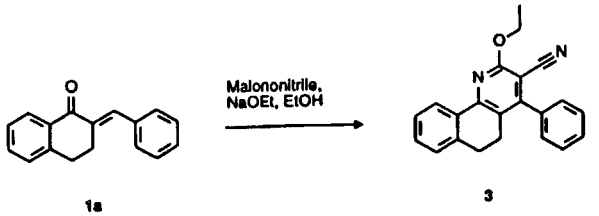

1a **3**

SCHEME 2

Subsequently, it was also demonstrated [5] that the pyran **2a** could rearrange under acidic conditions to the dihydropyridone **4** (Scheme 3).

2a **4**

SCHEME 3

Our interest was in the *N*-functionalization of pyrans such as **2b** and in particular the *N*-acetylation of such compounds. With the already described lability of this pyran nucleus under basic and acidic conditions, we were concerned that under typical acetylation conditions (acetyl chloride, pyridine, DMF, room temperature, several days) there could be scope for related undesired rearrangements to occur. The exciting antiproliferative activity [6] of this series made an unambiguous structural assignment of fudamental importance (the product of the acetylation of pyran **2b** had an IC_{50} of less than 10 nanomolar against the concanavalin A induced proliferation of rat spleen T-cells). It was, therefore, necessary to distinguish between two potential pathways (Scheme 4), one involving the desired *N*-acetylation, the other involving O-acetylation of a dihydropyridone formed by rearrangement of **2b**.

Results and Discussion.

Pyran **2b** was prepared from 7-methoxy-1-tetralone **7** according to Scheme 5. The structural assignment of the acetylation product, **5a** or **6a** (Scheme 4), required determination of the relative position of the N and O atoms. Preparation of an *N*-methyl derivative **5b** or **6b** (Scheme 4), facilitated the nmr investigation by providing a "proton probe" attached to one of these heteroatoms. Two complementary nmr strategies were then followed to study the structural effect of this methylation; (i) 1-Dimensional Nuclear Overhauser Effect (nOe) difference spectroscopy, to investigate the spatial environment of the NMe protons,

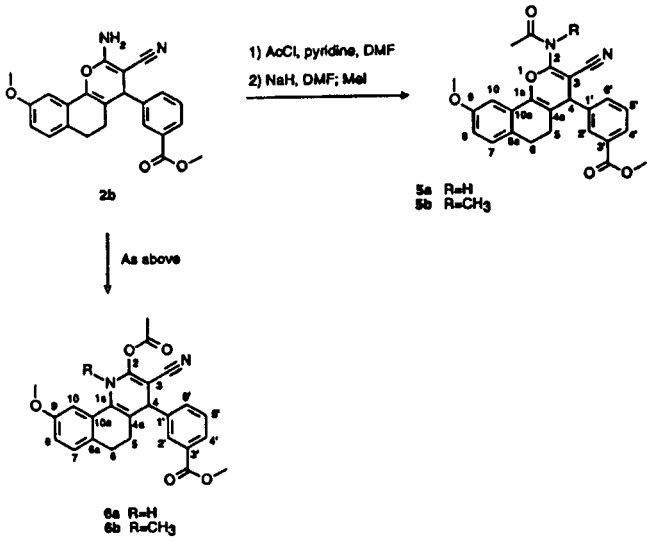

SCHEME 4

and (ii) ^{13}C nmr studies using chemical shift comparisons of the acylated product with its NMe derivative and analysis of long range C-H coupling from the *N*-Me protons.

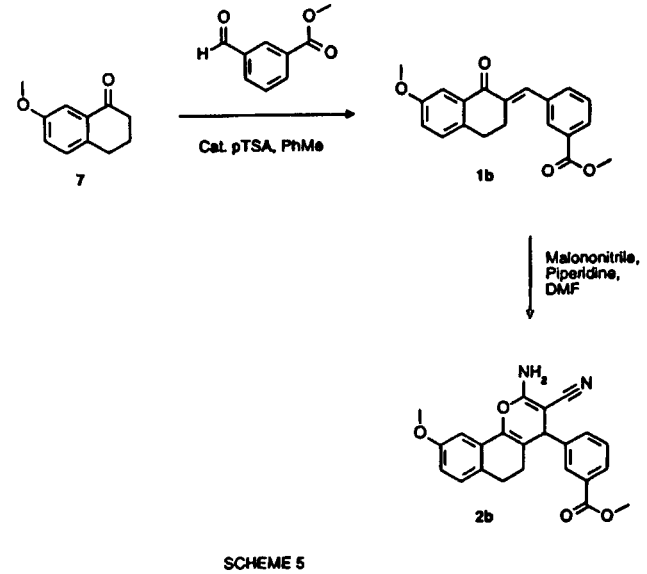

SCHEME 5

1D nOe Experiments on *N*-Me Derivative **5b** or **6b**.

The ^1H nmr spectrum of the *N*-Me component **5b** or **6b** was assigned (Table 1) by analysis of coupling patterns and chemical shift comparisons with simple model compounds. Comprehensive nOe experiments then provided the following significant data: Irradiation of 10CH (*ca.* 90% saturation) produced a medium strength positive nOe at 9-OMe (1.7%) and weak enhancements at the -NMe (0.3%) and MeCO- (0.3%). Similarly, saturation of -NMe, MeCO- or 9-OMe (all *ca.* 90% saturation) produced 2.5%, 1.7% and 11.1% enhancements at H-10 respectively. Both NMe and MeCO groups also gave weak enhancements (<2%) to aromatic protons in the phenyl ring (H-2' and H-6'), with slightly more intense effects being apparent from the MeCO- protons.

Table 1

^1H (300 MHz) and ^{13}C (75 MHz) NMR Spectral Data for **2b**, **5a** and **5b**

Atom	Proton (δ ppm)			Carbon (δ ppm)		
	2b	**5a**	**5b**	**2b**	**5a**	**5b**
C-1a				139.3	140.2	140.7
C-2				159.4	151.1	155.4
C-3				55.3	80.8	86.8
C-4	4.24 s	4.56 s	4.70 s	41.5	42.4	42.7
C-4a				111.1	111.3	110.9
C-5	2.17 m	2.24 m	2.23 m	24.0	23.8	23.9
	1.80 m	1.86 m	1.87 m			
C-6	2.67 m	2.71 m	2.73 m	25.2	25.1	25.1
	2.52 m	2.55 m	2.57 m			
C-6a				126.4	126.4	126.5
C-7	7.08 d	7.11 d	7.13 d	*	*	*
C-8	6.82 dd	6.85 dd	6.87 dd	112.6	112.8	113.0
C-9				157.5	157.6	157.6
C-10	7.14 d	7.03 d	6.98 d	106.5	106.7	106.5
C-10a				128.5	*	127.9
C-1'				144.0	141.8	141.0
C-2'	7.85 t	7.94 t	7.99 t	*	*	*
C-3'				129.4	129.7	129.8
C-4'	7.88 dt	7.93 dt	7.96 dt	*	*	*
C-5'	7.52 t	7.52 t	7.61 t	128.6	128.9	129.2
C-6'	7.56 dt	7.65 dt	7.73 dt	132.2	132.4	132.5
CN				119.7	116.2	115.3
9-OCH_3	3.78 s	3.77 s	3.77 s	54.6	54.7	54.7
3'-$OCOCH_3$	3.85 s	3.86 s	3.86 s	51.6	51.6	51.7
3'-$OCOCH_3$				165.6	165.4	165.4
2-$NCOCH_3$		2.09 s	2.31 s		22.5	20.6
2-$NCOCH_3$					167.9	168.5
2-NCH_3			3.20 s			33.3
*				127.6	128.0	128.4
				127.7	127.9	128.2
				127.4		128.1

Molecular Modelling.

All structures were arbitrarily modelled as the S enantiomer. After initial minimization it was clear that there could be at least two ring pucker options about the C4a-C5-C6-C6a axis which are influenced by the orientation of the pendant phenyl group at C4. Moving C5 and C6 to different starting positions for minimization simply induced the opposite pucker and opposite orientation of the phenyl ring. Hence, it was clear that only one basic pyran **5** or basic dihydropyridine **6** skeleton needed to be examined. Semi-empirical studies using PM3 on the dihydropyridine **6b** showed the C3-C2-N-C dihedral angle to be -113.9° and the C4a-C1a-N-C dihedral angle, 110.7°. An even flatter geometry was obtained with the AM1

be -113.9° and the C4a-C1a-N-C dihedral angle, 110.7°. An even flatter geometry was obtained with the AM1 Hamiltonian, C3-C2-N-C being -128.4° and C4a-C1a-N-C being 123.1°. For the molecular mechanics and conformational search calculations a nitrogen atom type which closely mimicked these semi-empirical torsion angles was therefore required. A CHARMm NP atom type was therefore selected which gave a C3-C2-N-C dihedral of -134.9° and a C3-C2-N-C dihedral of 127.7°. The low energy structures and interatomic distances of interest for each structure will be dealt with in turn.

Pyran **5b**.

Various types of systematic conformational searches about the O1-C2-N-CO and C2-N-CO-C torsions were executed which identifed two minima, the lowest energy conformation is shown in Figure 1. The barrier to transition between these two minima was ~10 kcal. Dummy atoms were placed at the mid point of the protons on the methyl groups and distances from the C10 proton to the dummy atoms measured. Over a 1 kcal energy range from the 'global minimum' the NCH_3-10CH distance was 4.8 ±0.3 Å and the $COCH_3$-10CH distance was 4.7 ±0.5 Å. In the other minima the distances were NCH_3-10CH, 5.3 ±0.3 Å and $COCH_3$-10CH, 3.8 ±0.3 Å. In all cases the low energy conformations gave the 10CH - $9CH_3O$ distance to be 3.5 Å with the methoxy group at ~90° to the phenyl ring.

Dihydropyridine **6b**.

In a two bond conformational search about the N-C2-O-CO and C2-O-CO-O bonds a much more complex series of minima was observed than was seen for the pyran with many small local minima. However, two principal areas of low energy conformational space were established and the lowest energy structure is shown in Figure 1. The largest area of low energy conformational space described contains the 'global minimum' structure, although this is only 1 kcal below the lowest energy structure found in the other principle minima. The barrier to transition between these two areas was found to be 7.9 kcal. The NCH_3-10CH distance for both of these minima is consistent, being 2.7 ± 0.2 Å. The $COCH_3$-10CH distance though is considerably shorter for the 'global minimum' (4.3 ±1.4 Å) than is observed in the other principle minima; 6.0 ±0.8 Å. Another minimum which represents a 180° rotation of the C2-O-CO-O torsion from the minimum energy conformation is also found. The $COCH_3$-10CH distance is 6.5Å and the NCH_3-10CH distance is 2.7Å. The $9CH_3O$-10CH distance is 3.5Å for all conformers.

From these data it is clear that in **6b** the 10CH-NCH_3 distance is significantly shorter than the $COCH_3$-10CH distance in both low energy conformations. Given these distances a 'strong' nOe should be expected at 10CH on

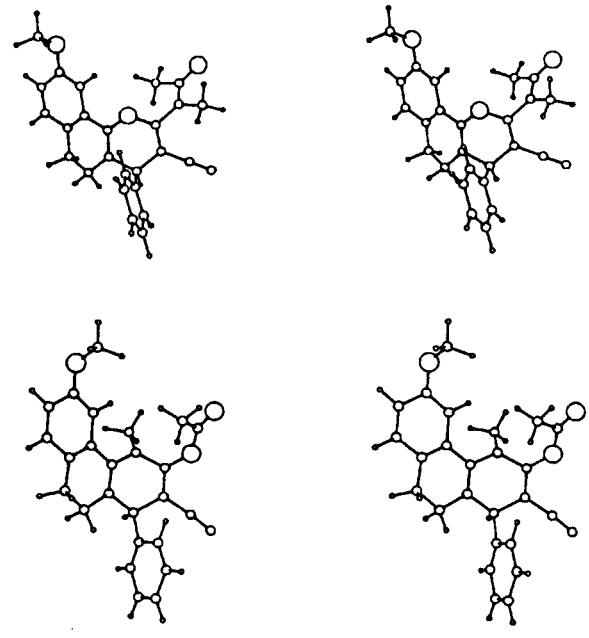

Figure 1. Stereoview of the lowest energy conformations of dihydropyran **5b** (top) and dihydropyridine **6b** (bottom).

irradiation of the NCH_3, compared to a 'weak' effect on irradiation of $COCH_3$. This is inconsistent with the observed nOe's. In contrast, the approximately equal effects experienced by 10CH upon irradiation of the NCH_3 or $COCH_3$ are consistent with the pyran **5b** in which both sets of methyl protons are greater than ~4.0Å from 10CH.

Approximations inherent in force field parametisation [7] and quantitative nOe analysis [8] are such that these experiments do not constitute an unambiguous structural proof. Therefore an independent verification of these findings was sought.

^{13}C NMR Experiments.

The ^{13}C nmr studies were applied in a two-step approach:

(i) Comparison of ^{13}C shifts of **5a** or **6a** around the "central" heterocycle before and after *N*-methylation was used in a qualitative sense to determine the site of the nitrogen atom.

(ii) Analysis of ^{13}C-^{1}H long range couplings from the *N*-Me protons to quaternary carbon centers then unambiguously assigned the pyran structure **5b**.

Step (i) required a full ^{13}C assignment of both components to enable a complete comparison. Protonated carbon centers were simply assigned (Table 1) by an inverse detected HMQC experiment [9]. However, a further 12 quaternary carbons remained, including the key heterocyclic ring centers. Their assignments relied primarily on HMBC experiments, an inverse detected correlation

incorporating a low pass J filter to suppress direct one-bond correlations, and with the $^{n}J_{CH}$ (n = 2, 3) evolution delay adjusted to 50 ms.

The HMBC spectrum of **5b** or **6b** immediately assigns the two C=O carbons and C-9 from their correlations to their attached, directly or *via* -O-, Me protons. Further assignments were, however, complicated by the potential detection of both ^{2}J and ^{3}J couplings. To illustrate this point part of the HMBC spectrum is shown in Figure 2. Clearly, H-4 shows all of the nine possible 2 or 3 bond correlations to quaternary and protonated carbons. Comparison with a proton coupled carbon spectrum (data not shown) indicates that the HMBC experiment may detect couplings of 2 Hz or less. For example, the H-4 to 3-CN coupling was measured as 2.5 Hz (sharp doublet in coupled spectrum) and this correlation is clearly seen in Figure 2.

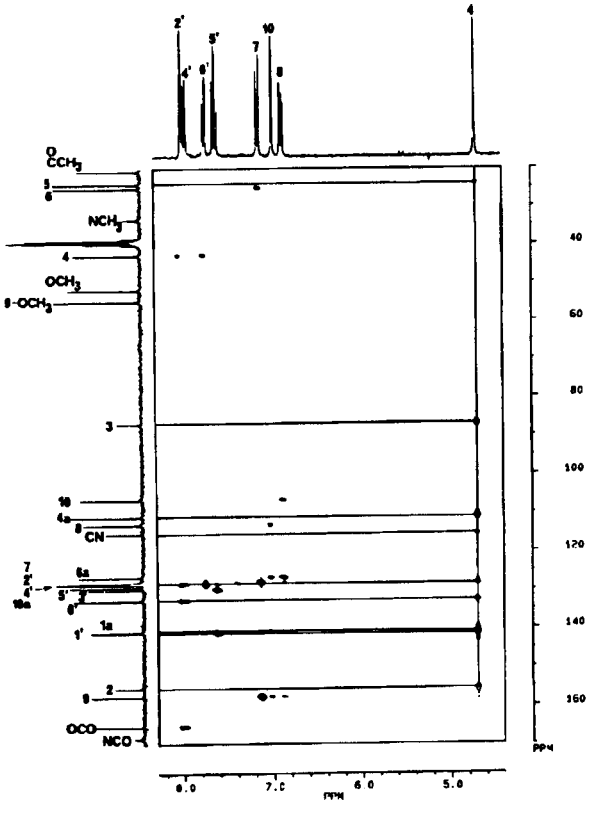

Figure 2. Part of the contour plot of the proton detected HMBC spectrum of **5b** showing correlations from aromatic protons and the ring methine proton (H-4).

In general, all the aliphatic protons showed connectivities over both 2 and 3 bonds, and carbon assignment ambiguities could only be resolved by comparing correlations from several different protons (Table 2). For example; C-4a correlates to H-4 (^{2}J), CH_2-5 (^{2}J) and CH_2-6 (^{3}J,), compared to C-1a which correlates to H-4 (^{3}J), CH_2-5 (^{3}J) and H-10 (^{3}J). In contrast, the aromatic protons (Table 2) only show strong 3 bond correlations (as expected when considering the relative sizes of ^{2}J and ^{3}J couplings in simple aromatic systems [11,12]), greatly facilitating the assignment process. The long range C-H correlations presented in Table 2 are thus sufficient to unambiguously assign all of the quaternary carbons.

In addition, several of the key heterocyclic ring carbons were independently assigned (prior to the HMBC data becoming available) by 1D heteronuclear nOe experiments. For example, presaturation of the H-4 proton resonance produced significant enhancements at C-4a, C-3 and C-1' as detected by difference spectroscopy (Figure 3). The nOe method provides a very satisfactory result in this case where the proton "target" is in an empty region of the spectrum. However, irradiation of key aromatic protons (*eg* H-10 to assign C-10a) was compromised to some extent by poor frequency selectivity in this more crowded proton region and, gave more ambiguous results. In addition, the experiments were particularly time-con-

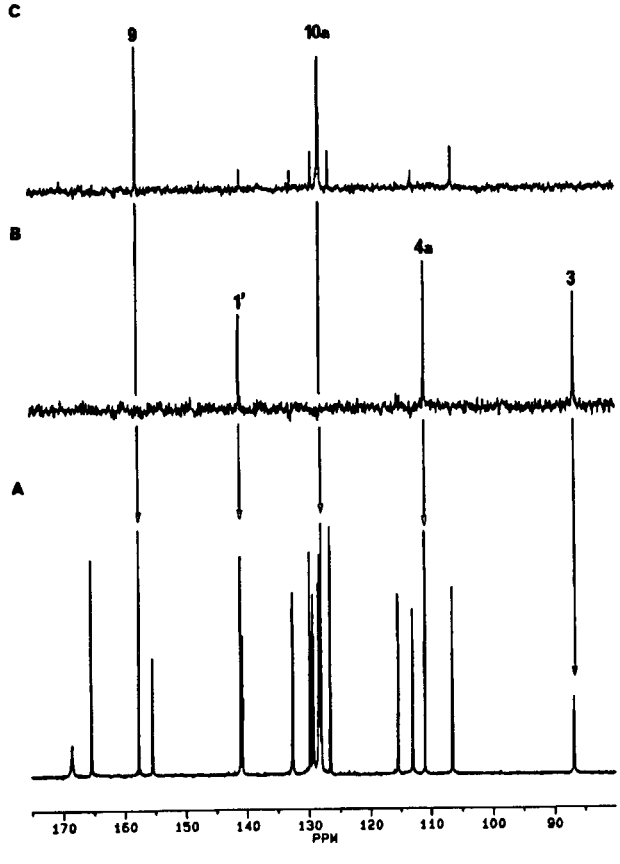

Figure 3. Heteronuclear nOe difference experiments performed on **5b**: a) Control spectrum, b) Pre-irradiation of H-4, c) Pre-irradiation of H-10.

Table 2

Summary of HMBC Correlations Observed for Quaternary Carbons in **5b**

Carbon	Proton - 3 Bond Coupling	Proton - 2 Bond Coupling
C-1a	H-10, H-4, CH_2-5	
C-2	H-4, CH_3N	
C-3		H-4
C-4A	CH_2-6	H-4, CH_2-5
C-6A	H-8, H-10, CH_2-5	CH_2-6
C-9	H-7, 9-OCH_3	H-8, H-10
C-10A	H-7, CH_2-6	
C-1'	H-5'	H-4
C-3'	H-5'	
CN	H-4	
NC=O	CH_3N	CH_3CO
OC=O	H-2'/H-4', CH_3O-	

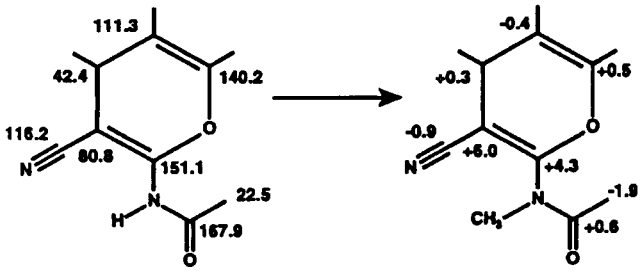

Figure 4. ^{13}C shifts of heterocyclic ring carbons in **5a** and the shifts experienced upon *N*-methylation to give **5b**.

suming when compared to the HMBC technique.

Evidence for the pyran structures **5a** and **5b** is now apparent on considering the effect of *N*-methylation on the hetero-ring carbon shifts (Table 1 and Figure 4). As expected, methylation results in significant deshielding for only C-2 and C-3 in the pyran ring. In the dihydropyridine alternatives **6a** and **6b** C-4a and C-1a would be expected to mirror the substitution trends for C-2/3 rather than give the minimal effects actually observed.

Final and conclusive assignment of the pyran structure came, however, from the HMBC spectrum of **5b**. A small region of the spectrum (F1 = low field carbons, F2 = methyl protons) is shown in Figure 5 at a contour level which contains only the strong correlations from the four methyl singlets. The *N*-Me protons show long range couplings to both C-2 and to the C=O, confirming an exocyclic *N*-acyl structural unit. The dihydropyridine **6b** would require an unprecedented 5-bond coupling to account for this correlation.

In summary, a preliminary combination of conformational analysis and semi-quantitative nOe investigations

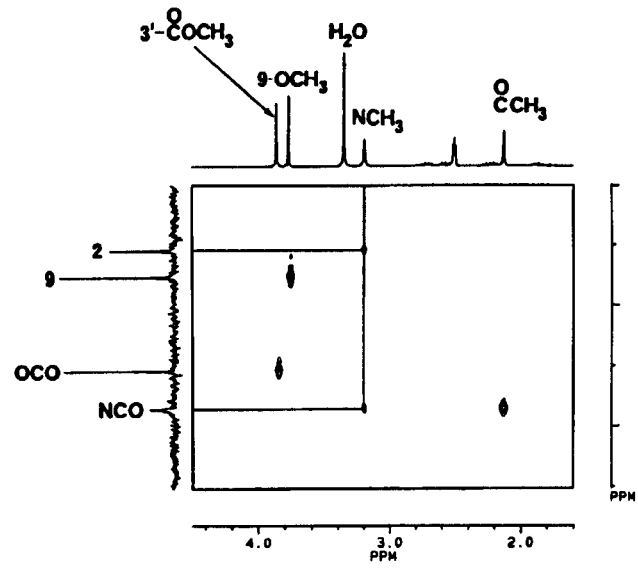

Figure 5. Expansion of the HMBC spectrum of **5b** showing correlations from the four methyl singlets to the low field carbon region.

was used to distinguish between the probable structural isomers **5b** and **6b**. Verification of these results was provided by analysis of long range proton-carbon couplings detected by the HMBC experiment.

EXPERIMENTAL

Melting points were determined on a Reichert hot stage apparatus and are uncorrected. The ir spectra were obtained as potassium bromide discs on a Bruker IFS 48 instrument. The uv spectra were obtained as methanol solutions using a Philips PU8725 instrument. Mass spectra were recorded on a VG7070E instrument. Microanalyses were carried out by the molecular structure research group at Eli Lilly and Company, Indianapolis.

Preparation of the Arylidenetetralone **1b**.

A stirred suspension of 7-methoxy-1-tetralone **7** (25.6 g, 145 mmoles), methyl 3-formyl benzoate (26.2 g, 160 mmoles) and toluene *p*-sulfonic acid monohydrate (0.5 g) in toluene (400 cm^3) was brought to reflux with separation of water. After 4 hours the solution was allowed to cool to room temperature and filtered to remove creamy needles of residual methyl 3-formyl benzoate. The filtrate was concentrated *in vacuo* to a red gum. This was crystallized yielding pale pink needles of the arylidenetetralone **1b** (31.0 g, 66%), m.p. 80-81° (ether/hexane). This was of sufficient purity for most purposes. An analytical sample was prepared by flash chromatography on silica gel with ethyl acetate/hexane (1:1) as eluant followed by recrystallisation (ether/hexane), mp 98°; ir ν max 1722 cm^{-1}; uv: λ max nm 226 (log ε 4.51) and 297 (4.26); ^1H nmr: δ 2.90 (2H, m), 3.11 (2H, m), 3.88 (3H, s), 3.95 (3H, s), 7.09 (1H, dd, *J* 8 and 3), 7.18 (1H, d, *J* 8), 7.51 (1H, t, *J* 8), 7.62 (2H, m), 7.86 (1H, s), 8.03 (1H, d,

J 7) and 8.12 (1H, s); ms: m/z 323 [(M + H)$^+$, 100%] and 263 (10).

Anal. Calcd. For $C_{20}H_{18}O_4$: C, 74.5; H, 5.6. Found: C, 74.5; H, 5.6.

Preparation of the Pyran **2b**.

To a stirred solution of the arylidenetetralone **1b** (14.3 g, 44.4 mmoles) and malononitrile (4.4 g, 66.6 mmoles) in DMF (150 cm^3) at ambient temperature was added dropwise piperidine (3 cm^3). The resulting black solution was stirred for 21 hours and then poured into water (500 cm^3). The product was extracted with dichloromethane (3 x 200 cm^3) and the combined extracts washed with water (2 x 200 cm^3), dried (magnesium sulfate), filtered and evaporated to yield a red gum. This was taken up in dioxane (100 cm^3) and diluted with water (250 cm^3). On standing overnight, a pink solid appeared. This was filtered off, washed with ethyl acetate and dried *in vacuo* at 110° providing methyl 3-[2-amino-3-cyano-9-methoxy-4*H*-5,6-dihydronaphtho[1,2-*b*]pyran-4-yl] benzoate **2b** (4.62g, 27%) as a pale yellow solid, mp 159-160°; ν max 2190, 1706 and 1680 cm^{-1}; ms: m/z 406 [(M+NH$_4$)$^+$, 53%], 389 [(M+H)$^+$, 94] and 253 (100).

Anal. Calcd. For $C_{23}H_{20}N_2O_4$: C, 71.1; H, 5.2; N, 7.2. Found: C, 70.8; H, 5.2; N, 7.1.

Acetylation of the pyran **2b**.

To a stirred, ice-cooled solution of the pyran **2b** (3.5 g, 9.0 mmoles) in DMF (100 cm^3) was added dropwise dry pyridine (4.4 cm^3, 54 mmoles) followed by acetyl chloride (3.85 cm^3, 54 mmoles). A heavy yellow precipitate appeared. The mixture was allowed to warm to ambient temperature and stirred for a further 24 hours. The black solution was poured into water (500 cm^3) and the resulting copious precipitate filtered off. After washing well with water and then with hexane, the solid was taken up in dichloromethane (500 cm^3) and stirred with neutral alumina (grade 3, 50 g) overnight. The mixture was concentrated to dryness and the solid placed onto a pad of neutral alumina (grade 3) on a large sintered glass funnel. Elution with dichloromethane/ether (1:1) yielded the product acetamide **5a** (1.30 g, 34%) as a crisp yellow solid mp 91-92°; ir: ν max 2192, 1723, 1696 and 1653 cm^{-1}; ms: m/z 448 [(M+NH$_4$)$^+$, 100%], 431 [(M+H)$^+$, 56], 430 (M$^+$, 62), 388 (36), 295 (23) and 253 (66).

Anal. Calcd. For $C_{25}H_{22}N_2O_5$: C, 69.8; H, 5.15, N, 6.5. Found: C, 69.5; H, 5.05; N, 6.3.

Methylation of the Amide **5a**.

To a stirred ice-cooled suspension of sodium hydride (50% dispersion, 67 mg, 1.4 mmoles) in dry DMF (10 cm^3) under nitrogen was added dropwise during 5 minutes a solution of the amide **5a** (0.50 g, 1.16 mmoles) in dry DMF (2 cm^3). The solution slowly went orange. After 45 minutes at ice-bath temperature, methyl iodide (1 cm^3) was added. The orange color faded to yellow and the ice-bath was removed. Two hours later, the solution was diluted with water (25 cm^3) and the product extracted with dichloromethane (3 x 20 cm^3). The combined organic extracts were washed with water (2 x20 cm^3), dried (magnesium sulfate) and evaporated to yield a yellow gum. This was chromatographed on neutral alumina (grade 3) with dichloromethane as eluant to yield the amide **5b** (0.37 g, 72%) as a pale yellow solid, mp 141-142°; ir: ν max 2218, 1724 and 1700 cm^{-1}; ms: m/z 462 [(M+NH$_4$)$^+$, 99%], 402 (64), 309 (7), 267 (100) and 163 (42).

Anal. Calcd. For $C_{26}H_{24}N_2O_5$: C, 70.3; H, 5.4; N, 6.3. Found: C, 70.2; H, 5.7; N, 6.1.

NMR Measurements.

The nmr spectra were recorded on solutions in *c.* 0.6 ml (methyl sulphoxide)-d_6 (Aldrich Chemical Company Limited, 99.9 atom %D) on a AM300 or AC300 Bruker spectrometer operating at 300.13 MHz for proton and 75.47 MHz for carbon observation. Typically data were obtained on 20 mg of sample in 5 mm tubes at 300K. Chemical shifts are reported relative to internal TMS.

1D ^{1}H NMR Spectra.

Typically proton nmr spectra were recorded with a sweep width of 6024 Hz in 16K real data points, giving an acquisition time of 2.7s and a digital resolution of 0.37 Hz/pt. The 1D nOe measurements were performed on a non-spinning sample using the Bruker microprogram NOEDIFF. The proton of interest was pre-irradiated for 3s followed by a 90° read pulse. Blocks of 16 scans preceded by 2 dummy scans were accumulated for each irradiation site, to give a total of 800 scans per site. No line broadening was applied prior to Fourier transformation.

^{13}C NMR Spectra.

Proton decoupled ^{13}C spectra were routinely recorded with a sweep width of 22000 Hz in 16K real data points, giving an acquisition time of 0.72s and a digital resolution of 1.4 Hz/pt. Exponential weighting with a line broadening factor of 2 Hz was applied prior to Fourier transformation. Proton coupled spectra were recorded in the gated decoupled mode with 32K real data points and no exponential weighting was applied prior to Fourier transformation. 1D ^{1}H-^{13}C nOe difference spectra were recorded on a concentrated sample (*c.* 100 mg in 0.6 ml). The proton of interest was pre-irradiated for 10s followed by a 90° ^{13}C read pulse; broadband proton decoupling was applied during data acquisition. Blocks of 64 scans preceded by 4 dummy scans were accumulated for each irradiation site to give a total of 2000 scans per site.

Proton Detected Heteronuclear Multiple Quantum Coherence (HMQC) Experiment.

The HMQC spectra were acquired on a Bruker AC300 spectrometer equipped with a dual ^{1}H/^{13}C 5mm probe with reversed geometry using the published sequence [9] which incorporates a BIRD [13] pulse to suppress ^{12}CH resonances. Typical parameter settings were 128 t_1 increments covering a spectral range of 2400 Hz in 2K data points using 48 scans and 2 dummy scans. The F1 dimension covered 13000 Hz. ^{13}C decoupling during acquisition was achieved by the GARP decoupling sequence [14]. Phase sensitive data were recorded using the TPPI method [15]. The data matrix was zerofilled to 4K and 512W in F2 and F1 respectively, and π/2 shifted sine-bell windows applied prior to double Fourier transformation.

Proton Detected Long-range Heteronuclear Correlation (HMBC) Experiment,

The published sequence was used [10]. Representative acquisition conditions were 160 scans (4 dummy scans) in 2K data points for each of 512 t_1 increments. Proton and carbon spectral widths were 2400 and 13000 Hz respectively. The data matrix was processed by zero-filling to 2K data points in F1 and 1K data points in F1, double Fourier transformation and a magnitude calculation. A π/2 shifted sine bell window was used in F1

and a sine-bell in F2.

Computational Details.

All molecular mechanics and conformational search calculations were carried out on either a Silicon Graphics 4D/320 GTX or an Indigo R3000. Model pyran **5b**, without 3' carboxy group and dihydropyridine **6b**, without 3' carboxy group structures were initially built in Quanta 3.3 [16] and minimised by a combination of steepest descent and adopted-basis Newton Raphson (ABNR) procedures to an energy gradient tolerance of 0.001 and an energy value tolerance of 0.0 using CHARMm 22 [16]. The 'move atom' facility was used to generate different starting geometries about the 4a-5-6-6a ring pucker before minimization. For the dihydropyridine an NP type nitrogen was selected. Reported missing angle parameters and estimated force constants were as follows:

Angle	Angle Value	Force Constant
NP-CUA1-OS	120.0	50.0
CUA1-NP-CUA2	120.0	66.3
CT-CUA1-CUY2	118.5	53.0
CUA2-CUA3-CUA2	119.6	51.9

Conformational searches were executed at 5° intervals through 360° about the O1-C2-N-CO bond in the case of the model pyran **5** and the N-C2-O-CO bond in the model dihydropyridine **6**. Two bond spins were executed through 360° at 15° intervals about the O1-C2-N-CO and C2-N-CO-C bonds in the pyran **5**, and the N-C2-O-CO and C2-O-CO-C bonds in the dihydropyridine **6**. Two types of calculation were run on these searches. Firstly, a 'fixed' search, where at each incremental change in angle the torsion is fixed and the rest of the structure subjected to 500 steps of ABNR minimization. Secondly, a 'relaxed search' was executed where the whole molecule is allowed to fully minimize through 500 steps of ABNR minimization after each incremental change in the torsion angle.
Semi-empirical calculations were carried out on a Cray-2 through MOPAC 6.0 [17] as implemented in Unichem 2.0 [18]. Both the AM1 and PM3 hamiltonians were used with full geometry optimization, and 100x normal precision.

Acknowledgements.

We would like to thank Dr. A. V. Geeson and Mr. P. J. Callow for the acquisition and interpretation of mass spectrometric data.

REFERENCES AND NOTES

[1] H.-H. Otto and H. Schmelz, *Monatsh. Chem.*, **110**, 115 (1979).
[2] H.-H. Otto, O. Rinus and H. Schmelz, *Monatsh. Chem.*, **110**, 249 (1979).
[3] M. M. Al-Arab, *J. Heterocyclic Chem.*, **26**, 1665 (1989).
[4] P. Victory, J. I. Borrell, A. Vidal-Ferran, C. Seoane and J. L. Soto, *Tetrahedron Letters*, **32**, 5375 (1991).
[5] H.-H. Otto and O. Rinus, *Arch. Pharm. (Weinheim)*, **312**, 548 (1979).
[6] European Patent Appl. 93301156.1/1992.
[7] W. G. Richards, ed. Computer-Aided Molecular Design, IBC Technical Services Ltd., London 1989, pp 23-41.
[8] D. Neuhaus and M. P. Williamson, The Nuclear Overhauser Effect in Structural and Conformational Analysis, VCH, New York, 1989.
[9] A. Bax and S. Subramanian, *J. Magn. Reson.*, **67**, 565 (1986).
[10] A. Bax and M. F. Summers, *J. Am. Chem. Soc.*, **108**, 2093 (1986).
[11] J. L. Marshall, Carbon-Carbon and Carbon Proton NMR Couplings: Applications to Stereochemistry and Conformational Analysis. Methods In Stereochemical Analysis, **Vol 2**, VCH, New York, 1983.
[12] P. E. Hansen, *Prog. Nucl. Magn. Reson. Spectrosc.*, **14**, 175 (1981).
[13] A. Bax, *J. Magn. Reson.*, **52**, 330 (1983).
[14] A. J. Shaka, P. B. Barker, and R. Freeman, *J. Magn. Reson.*, **64**, 547 (1985).
[15] D. Marion and K. Wuthrich, *Biochem. Biophys. Res. Commun.*, **113**, 967 (1983).
[16] QUANTA 3.3. MSI Ltd., Waltham, MA 02154 USA (1992).
[17] MOPAC 6.0. QCPE Bloomington, IN 47405 USA (1992).
[18] UNICHEM 1.1. Cray Research Inc., Eagan, MN 55121 (1992).